MODIFICATION OF THE TIME, FREQUENCY, AND SONAR IMAGE DOMAIN SIGNATURES OF CYLINDERS DUE TO A MATERIAL JUNCTION

T.D. Daniel NSWC-PCD, Panama City, Florida, USA

P.L. Marston Physics and Astronomy Department, Washington State University, Pullman, Washington, USA

1 INTRODUCTION

In this work we look at the enhanced back-scattering due to Rayleigh waves on cylinders. The geometry for a typical experiment is shown in Fig. 1a, the cylinder is rotated and back-scattered data is collected at a variety of aspects. All experiments here are mono-static with a co-located source/receiver. Previous work has studied the back-scatter enhancement due to Rayleigh waves on cylinders [1,2,3,5,4,6]. These back-scatter enhancements show up at specific aspect angles due to the criteria for coupling energy from the incident sound onto the target. For Rayleigh waves this coupling criteria can be written as a wave number matching criteria. Fig. 1b shows the relevant geometry where k_w is the wave number in water, k_m is the wave number in the material. Solving for the coupling angle, θ_R, and using the substitution $k_i = \omega/c_i$ gives,

$$\sin(\theta_R) = \frac{c_w}{c_R}, \tag{1}$$

where c_w is the sound speed in water and c_R is the phase speed of the Rayleigh wave in the material. A wave is launched on the cylinder when the normal to the cylinder's surface is tilted by θ_R relative to the direction of the incident sound. The Rayleigh wave speed, c_R, depends on the material properties and can be approximated by [7,8],

$$c_R = \frac{0.852 + 1.14\nu}{1+\nu} c_s, \tag{2}$$

where c_s is the shear speed in the material. The parameter ν is Poisson's ratio given by,

$$\nu = \frac{(c_l/c_s)^2 - 2}{2[(c_l/c_s)^2 - 1]}, \tag{3}$$

where c_l is the longitudinal speed in the material. We have expanded this study to brass cylinders and introduced a bi-metallic or compound cylinder that has a junction between two differing materials along the axis and will examine the affects of the juncion on the back-scattered signal. The affects of the material junction will be explored in three domains, aspect-angle/time, aspect-angle/frequency, and circular sythetic aperature sonar (CSAS) image. Table 1, collects the relevant wave speeds and coulping angles for the materials used.

It is typical to distinguish between three types of Rayleigh wave scattering contributions, helical, meridional, and face-crossing, based on how they traverse the cylinder. Helical waves spiral along the length, meridional waves run along the meridian of the cylinder, while face-crossing waves run back and forth along the flat faces. The interested reader should see Refs. 2, 3, and 9 for more information.

2 BRASS CYLINDER

Starting with the simpler single matrial cylinder case, Fig. 2a shows a circular scan of a 5:1 aspect ratio (diameter:length) brass cylinder. In the figure 0 degrees is end-on, where sound is incident

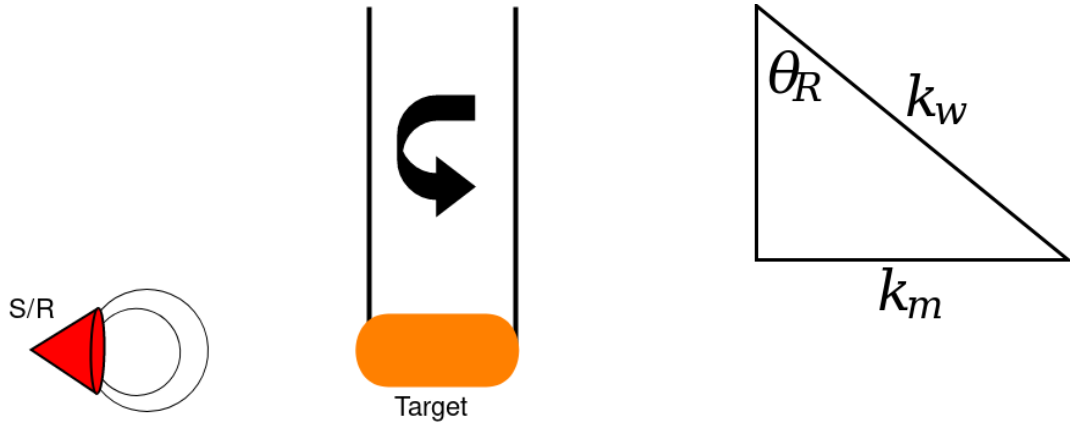

(a) The typical experimental geometry. The target is rotated through 360 degrees of aspect and back-scattered sound recorded.

(b) The wave number matching criteria requires the projection of k_w onto the surface of the cylinder match k_m to launch a wave. This allows us to draw the triangle shown in this figure and see that k_w and k_m are related by a fixed angle,θ_R.

Figure 1

normal to the end-cap, and 90 degrees is broadside, where the axis of the cylinder is perpendicular to the direction of the incident sound. Using the values for sound speeds in Table 1 the coupling angle for brass is $45°$. To couple into the face-crossing wave the cylinder must be tilted $45°$ off of end-on[3]. Similarly, to couple to the meridional wave the cylinder must be tilted $45°$ from broadside[1,2]. Since end-on and broadside are separated by $90°$ this means that the face-crossing and meridional wave will occur at the same aspect angle, though they will be separated in time provided the cylinder is not 1:1 aspect ratio.

Looking at Fig. 2a at $45°$ aspect there is an early back-scatter enhancement that corresponds to the face-crossing wave. At the same angle but later in time is a relatively late back scatter enhancement that comes from the meridional wave running down the length of the cylinder.

In the aspect-angle/frequency domain these two features overlap, as shown in Fig. 2b, there is only one strong feature halfway between end-on and broadside. Helical waves around broadside are also evident. This helical wave return is much stronger than in the previously studied aluminum case.

Finally, Fig. 3 shows the CSAS image of the brass cylinder. The meridional and face crossing waves appear near either end of the cylinder. These scattering phenomena appear as bright features in the image domain that make an angle of $45°$ with the respective surface they radiate from. In this case, since the angle is $45°$, they form a cross or an x. Helical waves are evident radiating outward from the cylinder at an angle of $45°$ relative to the horizontal.

3 COMPOUND CYLINDER

The compound cylinder target is a 5:1 (diameter:length) aspect ratio solid cylinder with 4 parts of the length being aluminum and 1 part brass. This makes the brass end a 1:1 apsect ratio cylinder and the aluminum end 4:1. Due to the symmetry of a single material cylinder only $90°$ of data is necessary to fully capture the scattering. This compound target breaks that symmetry and requires $180°$ of data to fully capture the scattring, due to the ends being different materials. The time-domain circular scan is shown in Fig. 4a. Zero degrees apsect in Fig. 4a corresponds to the aluminum end facing the acoustic source while $180°$ has the brass end facing towards the acoustic source. Looking

	Aluminum	Brass	Water
$c_l(mm/\mu s)$	6.420	4.536	1.485
$c_s(mm/\mu s)$	3.040	2.215	-
$c_R(mm/\mu s)$	2.920	2.069	-
θ_R	$\sim 30^\circ$	$\sim 45^\circ$	-

Table 1: Table of sound speeds and coupling angles for the materials of interest. c_l is the longitudinal speed, c_s the shear speed, c_R the Rayleigh speed, and θ_R the coupling angle for Rayleigh waves.

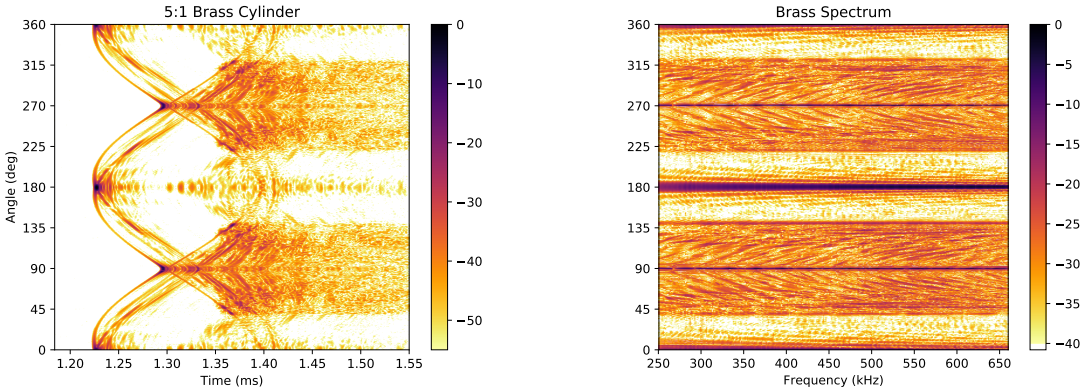

(a) Circular scan of the 5:1 brass cylinder. The data is shown in the aspect-angle/frequency domain. Shown at 0° is end-on and 90° is broadside. We are particularly interested in the meridional and face-crossing waves that show up at 45° aspect.

(b) The aspect-angle/frequency domain for the brass cylinder. In this domain we lose all time resolution and so the meridional and face-crossing wave are overlapped in both angle and frequency. These waves show themselves as features 45° between end- on and broadside.

Figure 2

near 90° aspect in Fig. 4a we see a lack of symmetry around broadside as expected. The aspect-angle/frequency domain, shown in Fig. 4b, has features at 45° and 30° from end-on and broadside corresponding to the brass and aluminum Rayleigh waves, respectively. The brass meridional and face crossing waves are superposed in both the time domain, since the coulping angle is 45° and the brass end is 1:1, and in the frequency domain.

There are four distinct backscattered returns in the full 360° scan that have interacted with the material junction. The meridional wave on the aluminunm end of the cylinder, when it is closer to the acoustic source than the brass, will reflect off the material junction. This happens twice in the full scan, 30° to one side of the broadsides. These aluminum returns are circled in Fig. 5 and corrspond to the lower green circle and upper black circle. There are similar returns from the meridional wave on brass that interacti with the material junction, also circled in Fig. 5 with the blue and lower black circle.

The brass and aluminum meridional waves that interact with the material junction show up in the image domain as a diamond structure offset from the center of cylinder, circled in Fig. 6a. Fig. 6b has a vertical line drawn where the junction is on the cylinder splitting the diamond. The left hand side of the structure is made of the two aluminum meridional wave returns, indicated by the 30° angle made with the horizontal. While the bras meridional waves make up the right side of the diamond, they make a 45° with the horizontal.

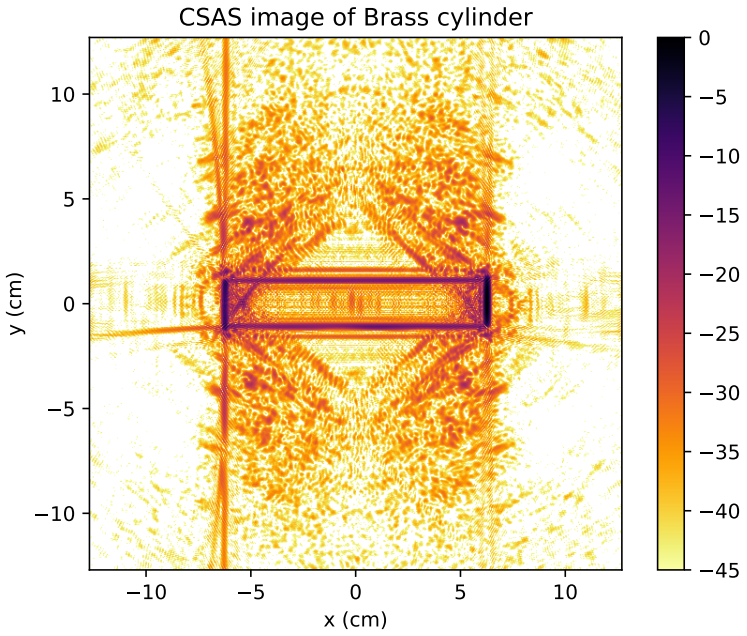

Figure 3: CSAS image of the brass cylinder. The face-crossing and meridional waves show up near the end caps in the image. Since the coupling angle is 45° these features show up as a cross or an x in the image. Radiating out from the cylinder we can see the helical waves.

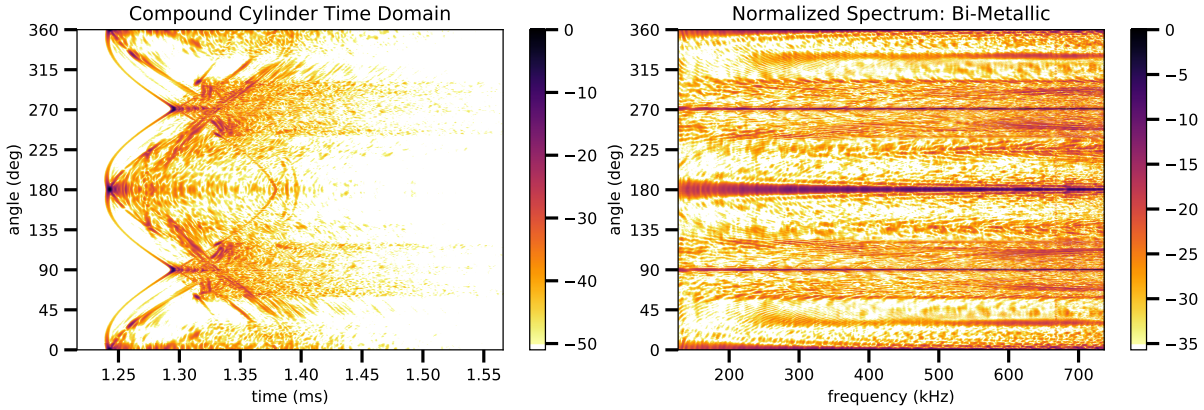

(a) The aspect-angle/time domain data for the compound cylinder. For a typical cylinder you only need 90° of data due to the symmetry. This target breaks that symmetry and so we have to take at least 180° of data. This is easily seen by looking at broadside, near 90°. Broadside is not symmetric in aspect-angle

(b) The aspect-angle/frequency domain of the compound cylinder. This spectrum looks roughly like a combination of the previous brass and aluminum spectra. We can see the aluminum face-crossing wave at 30° off the aluminum end-on. 45° off the brass end-on we can see features associated with both the meridional and face- crossing wave.

Figure 4

This associaton of the aluminum and brass waves with the left and right of the diamond is made clear if the individual returns circled in Fig. 5 are windowed and imaged. This leaves a clean image with only the contributions from the desired returns. Fig. 7a shows the image domain including only the green and blue circled reagions in Fig. 5. The brass and aluminum features map to opposite sides of

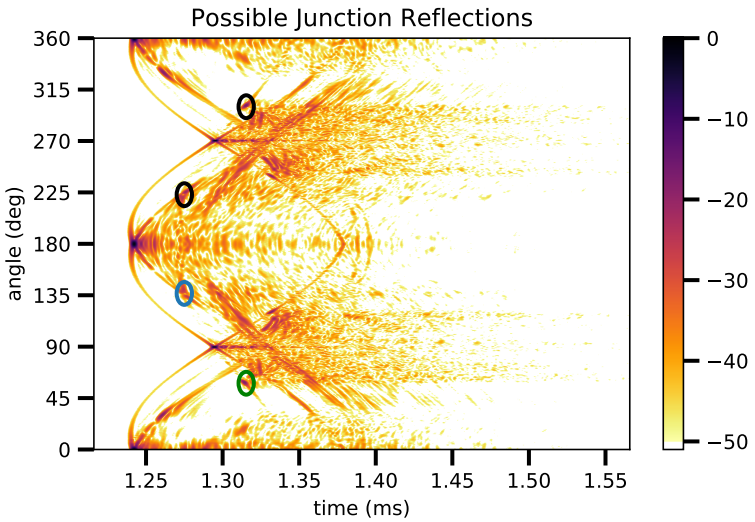

Figure 5: The aspect-angle/time domain of the compound cylinder. The circles indicate various features of interest that will be isolated and imaged independently. The green circle is a single aluminum meridional wave associated with the junction. The blue circle is one of the brass features. It contains both the face-crossing and meridional wave features since the brass end is 1:1. This target is symmetric around $180°$ ***aspect angle so these features both occur twice, the second occurrence of each is circled in black.***

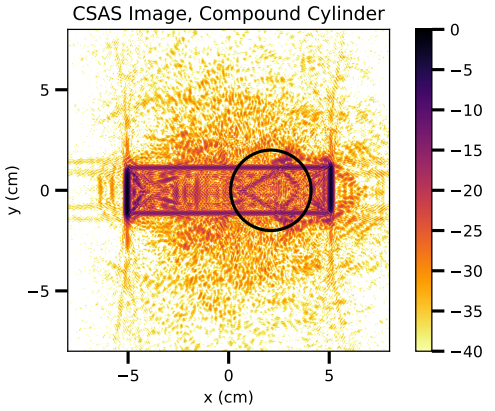

(a) CSAS image of the compound cylinder. The interesting diamond-like structure on the interior of the image is circled for emphasis.

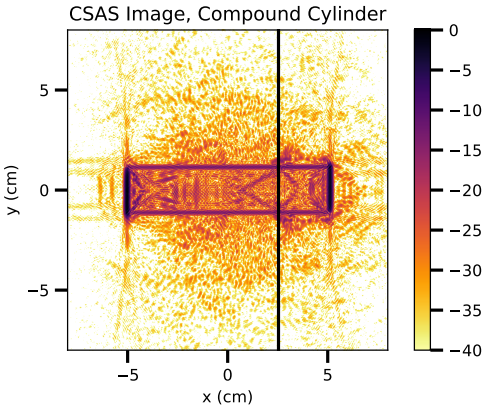

(b) CSAS image of the compound cylinder. Here we have added a vertical line where the material junction should be. It splits the interior diamond structure giving further indication that this feature is associated with the junction.

Figure 6

the junction, idicated by the vertical line, with the aluminum to the left and the brass to the right. If all four of the circled regions in Fig. 5 are included Fig. 7b is produced with the full diamond present. It is worth noting that the brass meridional and face crossing waves that were overlapping in both the time and frequency domains have been separated in the image with the face crossing waves radiating from what would be the brass face of the cylinder.

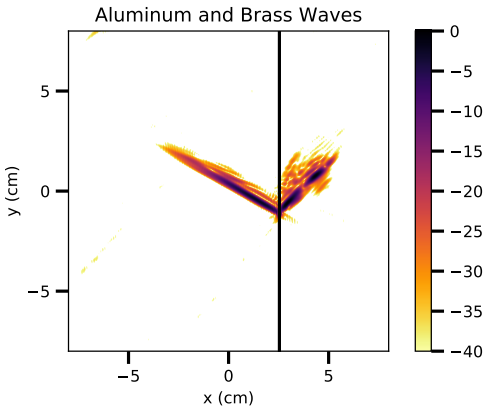

(a) CSAS image that includes both the green and blue circled regions in Fig. 5. This includes one of each of the brass and aluminum features that reflect off the junction. In this image it is easy to see how these features map to opposite sides of the junction and form different angles with horizontal.

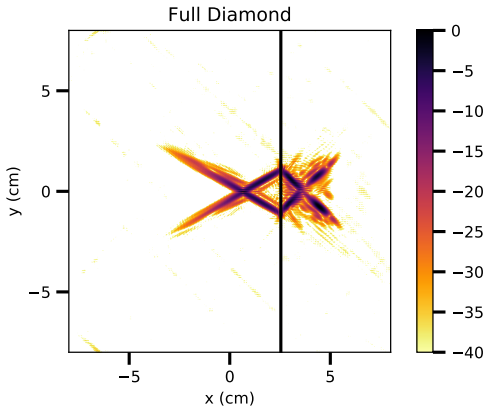

(b) CSAS image including all the region circled in Fig. 5. We see the full diamond feature. The left hand side is made up of the aluminum meridional waves that reflect off the junction, while the right hand side is formed by the brass meridional waves. In this image it is easy to see that the two sides come from the junction and that the two halves are not symmetric. The aluminum and brass features are at different angles from the horizontal.

Figure 7

4 CONCLUSION

Using our knowledge of the simple cylinder cases and how the meridional and face- crossing waves manifest in each domain we have been able to interpret the effect of the junction between on the compound cylinder. The waves that interact with the junction will scatter earlier than if they had to run the full length of the cylinder. This early scattering breaks the four-fold symmetry of a simple cylinder and forces the acquisition of $180°$ of data collection to fully capture the scattering. With the brass end of the cylinder being 1:1 aspect ratio this early scattering from the junction means the face-crossing and meridional wave overlap in both time and apect-angle. They can be sucessfully separated by imaging. The meridional waves that interact with the junction show up in the image domain as a diamond structure centered around the material discontinuity. The different ends of the cylinder can be identified in the image domaine based on the angle the features make with the horizontal, which matches the coupling angle of the wave for each material. Windowing in the aspect-angle/time domain serves to isolate features of interest and allows imaging of just the desired regions. This type of distinctive feature has application in target descrimination.

5 ACKNOWLEDGMENTS

The Washington State University component of this reasearch was supported by the U.S. Office of Naval Research under Awards No. N000141512603 and N000141912039.

REFERENCES

1. Philip L. Marston. Approximate meridional leaky ray amplitudes for tilted cylinders: End-backscattering enhancements and comparisons with exact theory for infinite solid cylinders.

The Journal of the Acoustical Society of America, 102(1):358–369, July 1997. ISSN 0001-4966. doi: 10.1121/1.421010.

2. Karen Gipson and Philip L. Marston. Backscattering enhancements due to reflection of meridional leaky Rayleigh waves at the blunt truncation of a tilted solid cylinder in water: Observations and theory. *The Journal of the Acoustical Society of America*, 106(4):1673–1680, August 1999. ISSN 0001-4966. doi: 10.1121/1.427917.
3. Karen Gipson and Philip L. Marston. Backscattering enhancements from Rayleigh waves on the flat face of a tilted solid cylinder in water. *The Journal of the Acoustical Society of America*, 107:112–117,(2000). doi: 10.1121/1.428295.
4. Mario Zampolli, Aubrey L. Espana, Kevin L. Williams, Steven G. Kargl, Eric I. Thorsos, Joseph L. Lopes, Jermaine L. Kennedy, and Philip L. Marston. Low- to mid-frequency scattering from elastic objects on a sand sea floor: Simulation of frequency and aspect dependent structural echoes. *Journal of Computational Acoustics*, 20(02):1240007, May 2012. ISSN 0218-396X. doi: 10.1142/S0218396X12400073.
5. Kevin L. Williams, Steven G. Kargl, Eric I. Thorsos, David S. Burnett,Joseph L. Lopes, Mario Zampolli, and Philip L. Marston. Acoustic scattering from a solid aluminum cylinder in contact with a sand sediment: Measurements, modeling, and interpretation. *The Journal of the Acoustical Society of America*, 127:3356-3371, 2010. doi: 10.1142/1.3419926.
6. Daniel S. Plotnick, Philip L. Marston, and Timothy M. Marston. Fast nearfield to farfield conversion algorithm for circular synthetic aperture sonar. *The Journal of the Acoustical Society of America*, 136(2):EL61–EL66, July 2014. ISSN 0001-4966. doi: 10.1121/1.4885486.
7. J. D. Achenbach. *Wave Propagation in Elastic Solids*. North-Holland Series in Applied Mathematics and Mechanics ; v. 16. North-Holland Pub. Co.; American Elsevier Pub. Co., Amsterdam, New York, 1973. ISBN 0-444-10465-8.
8. I. A. Viktorov. *Rayleigh and Lamb Waves: Physical Theory and Applications.* Ultrasonic Technology. Plenum Press, 1967. ISBN 0-306-30286-1.
9. Philip L. Marston. Spatial approximation of leaky wave surface amplitudes for three-dimensional high-frequency scattering: Fresnel patches and application to edge-excited and regular helical waves on cylinders. *The Journal of the Acoustical Society of America*, 102(3): 1628–1638, 1997. ddoi: 10.1121/1.420074.